Fault Tolerant Control for Aircraft Flaperon Faults Using Nonlinear Dynamic Inversion

Haripriya M.S
Department of Electrical Engineering
College of Engineering Trivandrum
APJ Abdul Kalam Technological University
Kerala, India
haripriyams01@gmail.com

Arlene Davidson R.
Department of Electrical Engineering
College of Engineering Trivandrum
APJ Abdul Kalam Technological University
Kerala, India
arlene@cet.ac.in

doi: https://doi.org/10.37285/bsp.SACAD2025.17

***Abstract*—This paper presents an advanced fault-tolerant control (FTC) framework tailored for the ATLANTE Remotely Piloted Aircraft (RPA), aimed at enhancing safety and reliability by addressing critical flaperon faults in aircraft control systems. The proposed FTC system combines two sophisticated approaches, Extended State Observer (ESO) and Nonlinear Dynamic Inversion (NDI), where ESO autonomously detects and estimates flaperon faults, supplying precise fault details. Leveraging these estimates, a robust control law is developed using the NDI technique, which compensates for faults by effectively managing the aircraft's complex nonlinear dynamics. This ensures precise control and stable performance under fault conditions. The effectiveness and feasibility of the proposed FTC framework are validated through comprehensive numerical simulations, designed to replicate various fault scenarios. The results demonstrate the system's robustness and fault tolerance, highlighting its potential to significantly improve the operational safety and reliability of the ATLANTE RPA. This framework offers a promising solution for fault management in advanced unmanned aerial systems.**

***Keywords*—Extended State Observer, Nonlinear Dynamic Inversion, Fault-Tolerant Control, Trajectory Tracking**

I. Introduction

The operational reliance on Unmanned Aerial Systems (UAS) for critical missions, such as those performed by the ATLANTE tactical Remotely Piloted Aircraft System (RPAS) [1], [2], necessitates unparalleled levels of safety and reliability. These aircraft exhibit complex, nonlinear dynamics—including aerodynamic stalls, actuator saturation, and significant cross-coupling—which complicate control design and can amplify the impact of system faults. Flaperon faults are especially critical, as they directly compromise both lift and roll control, posing a severe threat to flight stability. This paper addresses this specific vulnerability by developing a dedicated fault-tolerant control (FTC) framework for the ATLANTE RPA, aiming to enhance its resilience against flaperon failures.

The foundation of effective FTC rests on robust Fault Detection and Diagnosis (FDD). A significant body of research leverages advanced observers for this task. Sliding Mode Observers (SMOs) are widely recognized for their robustness, enabling precise fault reconstruction in various scenarios, from oscillatory failures [3] to Linear Parameter-Varying (LPV) systems [4]. Adaptive SMOs further enhance this capability for real-time fault diagnosis [5]. Parallel to this, the Extended State Observer (ESO) framework has proven highly effective, capable of estimating and compensating for the combined effects of actuator faults and external disturbances, as demonstrated in quadrotor applications [6]. Further diversifying the field,Kalman Filtering techniques and data-driven approaches have been successfully applied. The Extended Kalman Filter (EKF) has been used for direct fault reconstruction in complex platforms like hex-rotor UAVs [7], while constrained Kalman filters effectively detect sensor and actuator faults by monitoring dynamic property changes [8]. Neural networks and statistical methods, such as adaptive RBFNN [9] and TFP-NARX modeling [10], provide additional powerful data driven fault detection capabilities. Other notable FDD strategies include subspace predictive control for real-time fault management [11] and online strategies using EKF-updated MLP networks [12].

Building upon FDD, the core of FTC lies in the control methodology. Research can be broadly categorized into several powerful strands. Adaptive and Robust Control techniques are prominent, with adaptive backstepping being integrated into FTC to handle model uncertainties and actuator faults for trajectory and flight-path control [13], [14]. The sliding mode control (SMC) paradigm, prized for its inherent robustness, has been extensively applied across various platforms and failure modes, including fault-tolerant control for Blended Wing-Body (BWB) aircraft [15], attitude control using synthetic jets [16], trajectory tracking for multirotor aircraft with PID surfaces [17], and specialized applications in engine and braking systems [18], [19].

Another major category involves Model-Based Reconfiguration and Control Allocation. Here, Nonlinear Dynamic Inversion (NDI) and its incremental variant (INDI) are key tools for managing nonlinear aircraft dynamics. Research spans from INDI for trajectory control [13] to online model identification and reconfiguration for structurally damaged aircraft [20], [21]. Restructurable guidance systems using EKF and Nonlinear Inverse Dynamics (NID) can stabilize damaged aircraft in gusty conditions [22]. For over actuated systems, adaptive control allocation methods are vital, dynamically redistributing control effort among healthy surfaces post-fault [23], [24]. Predictive Control strategies also offer a powerful model based approach, with studies exploring multiple model predictive schemes [25] and Model Predictive Control (MPC) for accident prevention [26], while probabilistic verification frameworks help select optimal configurations under severe faults [27].

The development of these advanced systems is underpinned by rigorous Aircraft Modeling and Simulation principles [28]– [31] and is validated through sophisticated simulation environments [32]–[35] that incorporate realistic elements like turbulence [34], [36], [37]. Virtual simulation platforms are essential for developing models for future real-time platforms [33], while comprehensive reviews of flight simulation techniques support realistic testing environments [32]. The journey toward real-world implementation also demands attention to certification and experimental verification, as addressed in work on certifiable control for V-tail aircraft [38], [39] and standardized procedures [40].

Within this context, the integrated ESO-NDI framework presented in [41] offers a streamlined and effective solution for fault-tolerant attitude tracking. This paper builds directly upon this approach, tailoring and rigorously evaluating the ESO-NDI combination to address the specific, critical challenge of flaperon fault tolerance in the ATLANTE RPA. Our contribution is the demonstration that this framework provides robust fault estimation and stable angular rate tracking, effectively managing the complex, multi-axis dynamics impaired by flaperon faults.

The main contribution of this paper lies in developing a Fault Tolerant Control (FTC) framework integrating an Extended State Observer (ESO) for flaperon fault estimation with a Nonlinear Dynamic Inversion (NDI) controller for compensation. The proposed method is validated on the ATLANTE Remotely Piloted Aircraft (RPA) using nonlinear dynamic inversion under varying fault conditions. The paper is organized as follows Section II presents the mathematical modeling of the aircraft dynamics. Section III describes the methodology, including the design of ESO and NDI controllers. Section IV provides simulation results and analysis, and Section V concludes the study with future research directions.

II. MATHEMATICAL MODELING

The dynamic model of the ATLANTE RPA is governed by force and moment equations

- Along the X-axis:

$$-mg\sin\theta + X_T + X_A = m(\dot{U} - RV + QW) \quad (1)$$

- Along the Y-axis:

$$mg\cos\theta\sin\phi + Y_T + Y_A = m(\dot{V} + RU - PW) \quad (2)$$

- Along the Z-axis:

$$mg\cos\theta\cos\phi + Z_T + Z_A = m(\dot{W} - QU + PV) \quad (3)$$

The moment equations about the body axes,

- About the X-axis:

$$L_T + L_A = (I_z - I_y)qr - I_{xz}pq + I_x\dot{p} - I_{xz}\dot{r} \quad (4)$$

- About the Y-axis

$$M_T + M_A = -(I_z - I_x)pr + I_{xz}(p^2 - r^2) + I_y\dot{q} \quad (5)$$

- About the Z-axis:

$$N_T + N_A = -(I_x - I_y)pq + I_{xz}qr + I_z\dot{r} - I_{xz}\dot{p} \quad (6)$$

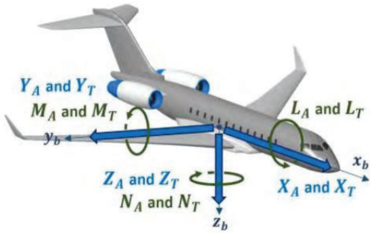

Fig. 1. Aerodynamic and propulsive forces and moments

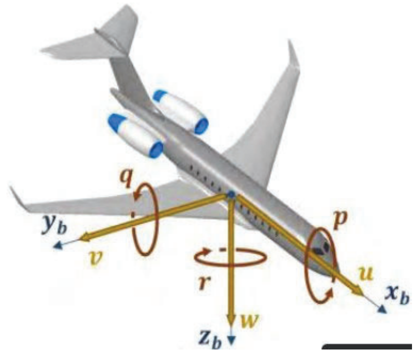

Fig. 2. Linear speeds and angular rates

Fig. 1 and Fig. 2 illustrate the aerodynamic and propulsive forces and moments, as well as the linear velocities and angular rates of the Atlante RPA, which are critical for implementing fault-tolerant control through ESO and NDI.

Aerodynamic Forces (X_A, Y_A, Z_A) Act along body frame X,Y,Z axes. Propulsive Forces (X_T,Y_T,Z_T) Thrust along X,Y,Z axes. Roll Moments (L_A,L_T) Affect roll about *X*-axis. Pitch Moments (M_A,M_T) Influence pitch about *Y* -axis. Yaw Moments (N_A,N_T) Control yaw about *Z*-axis.

Linear Velocities (U,V,W) Velocities in X,Y,Z directions. (p,q,r) Roll, pitch, yaw rates about X,Y,Z axes [41].

These illustrate the Atlante's nonlinear dynamics, critical for managing flaperon faults via ESO and NDI.

III. METHODOLOGY

The proposed methodology integrates fault detection and control reconfiguration into a unified framework. Initially, the ATLANTE RPA's dynamic model is simulated using force and moment equations. The Extended State Observer (ESO) detects and estimates actuator faults, while the Nonlinear Dynamic Inversion (NDI) controller compensates for these faults to maintain stable flight. The complete process from system initialization, fault detection, and controller adaptation is summarized in Fig. 3.

It commences at the "Start" node, initiating the aircraft control simulation. The first step, "Initialize Simulation" establishes the necessary initial conditions, parameters, and configurations for the simulation environment. This ensures the system is ready to model the aircraft's dynamic behavior accurately before proceeding to subsequent stages. In the next phase, the "Model System Dynamics" step simulates the aircraft's physical behavior, incorporating force and moment equations. Following this, the process reaches a pivotal decision node, "Fault = 0?", which evaluates whether the aircraft is operating without faults. This decision determines the control strategy, splitting the flowchart into two paths: normal operation using NDI or fault-tolerant control using FTC with ESO. If no faults are detected (Fault = 0), the system follows the left path for normal operation. The "Apply NDI Controller" step implements Nonlinear Dynamic Inversion to control the aircraft under standard conditions. The subsequent "Tune Controller Gains" step adjusts the controller parameters to optimize performance. The "Check for angular rates tracking" decision node then assesses whether the aircraft's angular rates (roll, pitch, yaw) are tracking the desired reference values accurately.

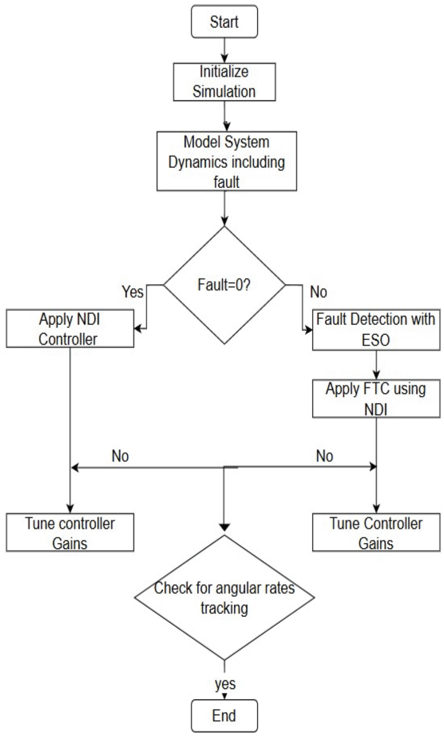

Fig. 3. Flowchart of Methodology

A successful track ("Yes") directs the process to the "End" block. If tracking fails ("No"), the process loops back to "Tune Controller Gains" for further adjustments, forming an iterative refinement loop. If faults are detected (Fault not 0), the system follows the right path for fault-tolerant control. The "Fault Detection with ESO" step employs an Extended State Observer to estimate the nature and magnitude of the faults, providing critical data for fault mitigation. Next, the "Apply FTC using NDI" step activates a fault-tolerant controller that adapts NDI principles to maintain control despite faults. The "Tune Controller Gains" step adjusts the controller parameters to optimize performance under these fault conditions. The second "Check for angular rates tracking" decision node checks if the angular rates are tracking correctly. If successful ("Yes"), the process terminates at the "End" block. If tracking is unsuccessful ("No"), the process loops back to "Tune the Controller Gains" for additional tuning, ensuring robust fault handling.

A. NDI Control law design for fault-free system

The design of the Nonlinear Dynamic Inversion (NDI) controller begins with the rotational dynamics of the aircraft, derived from the moment equations in Section II. For a fault-free system, the dynamics of the angular rate vector $\omega = [p \quad q \quad r]^T$ are governed by:

$$\dot{\omega} = F_1(\omega) + G_1(\omega)u_c \tag{7}$$

where:

- $F_1(\omega)$ is the nonlinear state-dependent term representing inherent rotational coupling effects
- $G_1(\omega)$ is the control effectiveness matrix
- $u_c = [L_T \quad M_T \quad N_T]^T$ is the vector of control moments (roll, pitch, yaw) in N·m
- ω and ω_d represent angular rates and desired angular rates Specifically, the nonlinear function $F_1(\omega)$ is defined as:

$$F_1(\omega) = \begin{bmatrix} \frac{(I_y - I_z)qr + I_{xz}pq}{I_x} \\ \frac{(I_z - I_x)pr - I_{xz}(p^2 - r^2)}{I_y} \\ \frac{(I_x - I_y)pq - I_{xz}qr}{I_z} \end{bmatrix} \tag{8}$$

The control effectiveness matrix is given by:

$$G_1(\omega) = \begin{bmatrix} \frac{1}{I_x} & 0 & 0 \\ 0 & \frac{1}{I_y} & 0 \\ 0 & 0 & \frac{1}{I_z} \end{bmatrix}, \quad G_1^{-1} = \begin{bmatrix} I_x & 0 & 0 \\ 0 & I_y & 0 \\ 0 & 0 & I_z \end{bmatrix} \tag{9}$$

The control objective is to track a desired angular rate profile $\omega_d(t)$. desired trajectory and its derivative are specified as:

$$\omega_d(t) = \begin{bmatrix} 0.1 \\ 0.5 \\ -0.1 \end{bmatrix} \sin(0.1t), \dot{\omega}_d(t) \begin{bmatrix} 0.1 \\ 0.5 \\ -0.1 \end{bmatrix} 0.1\cos(0.1t) \tag{10}$$

The tracking error is defined as:

$$e = \omega_d - \omega \tag{11}$$

The angular–rate tracking error e represents the difference between the desired angular rate ω_d and the measured angular rate ω.

$$v = \dot{\omega}_d + K_p e + K_d(\dot{\omega}_d - \dot{\omega}) \tag{12}$$

The pseudo–control input v represents the desired angular acceleration.

$$\dot{e} + \frac{K_P}{1 + K_d} e = 0 \tag{13}$$

Substituting the pseudo–control from Eq.(12) into the closed–loop dynamics yields the first–order stable error dynamics shown above, ensuring exponential convergence of the tracking error to zero.

$$\dot{\omega} = F_1(\omega) + G_1(\omega)u_c \tag{14}$$

The aircraft's angular–rate dynamics are modeled by $F_1(\omega)$, which includes the nonlinear aerodynamic and inertial effects, and $G_1(\omega)$,the control effectiveness matrix that maps the control inputs u_c to the angular accelerations.

$$u_c = G_1{}^{-1}(\dot{\omega}_d + K_p e + K_d(\dot{\omega}_d - \dot{\omega}) - F_1(\omega)) \quad (15)$$

This control law enables precise tracking of desired angular rates under nonlinear dynamics.

Table shows the parameter values [6]

TABLE I
AIRCRAFT PARAMETERS [6]

Parameter	Value
Mass(m)	570kg
Gravity(g)	9.81m/s²
Inertia(Ix)	1342kg·m²
Inertia(Iy)	1386kg·m²
Inertia(Iz)	1952kg·m²
Product of Inertia(Ixz)	51kg·m²
Thrust (FTX)	600N
Thrust (FTY)	200N
Thrust (FTZ)	150N
Roll Moment (LT)	171Nm
Pitch Moment (MT)	149Nm
Yaw Moment (NT)	206Nm
Forward Speed(u)	37.5m/s

B. Design of Extended State Observer

Flaperon faults in the ATLANTE RPA affect roll, pitch, and yaw rates ($\omega = [p,q,r]^T$), which are measured by onboard sensors, but actuator faults ($f_a = [f_{a,p}, f_{a,q}, f_{a,r}]^T$) are not directly measurable.

The angular rate dynamics under faulty conditions are modeled as:

$$\dot{\omega} = F_1(\omega) + G_1(\omega)(u_c + f_a) \quad (16)$$

where $F_1(\omega)$ and $G_1(\omega)$ are as defined in Eqs. (8) and (9) , and $u_c = [L_T, M_T, N_T]^T$ represents the commanded control moments

The ESO augments the state as, $z = [\omega^T \quad f_a^T]^T$ with dynamics:

$$\dot{z} = \begin{bmatrix} F1(\omega) + G1(\omega)(u_c + f_a) \\ 0 \end{bmatrix} \quad (17)$$

The ESO estimates $\hat{z} = [\hat{\omega}^T \quad \hat{f}_a^T]^T$: $\dot{\hat{z}}$

$$= \begin{bmatrix} F1(\hat{\omega}) + G1(\hat{\omega})(u_c + \hat{f}_a) \\ 0 \end{bmatrix} + L(\omega_m - \hat{\omega}) \quad (18)$$

where ω_m is the measured angular rate, and $L = [L_1^T \quad L_2^T]^T$ is the observer gain matrix. The implementation involves:

1) Initialize: $\hat{\omega} = \omega_m$, $\hat{f}_a = 0$
2) Compute $F_1(\hat{\omega})$, $G_1(\hat{\omega})$

$$\dot{\hat{\omega}} = F1(\hat{\omega}) + G1(\hat{\omega})(u_c + \hat{f}_a) + L_1(\omega_m - \hat{\omega}) \quad (19)$$

$$\dot{\hat{f}}_a = L_1(\omega_m - \hat{\omega}) \quad (20)$$

Gains L_1, L_2 are tuned to ensure convergence, enhancing fault detection reliability. A fault injection mechanism simulates actuator degradation and disturbances across three control channels to evaluate ESO robustness:

1) **No Fault** ($t(k) \leq 20$s): $\Lambda(:,k) = [0;0;0]$, $f_{osc} = [0; \quad 0; \quad 0;]$
2) **Ramp-Up** ($20 < t(k) \leq 30$s):
   Loss factor $\lambda = 0.5 \cdot (\frac{t(k)-20}{10})$, $\Lambda(:,k) = [\lambda;\lambda;\lambda]$;
   Oscillatory disturbance,
   $f_{osc} = [30;30;30] \cdot \sin(2\pi \cdot 0.5 \cdot (t(k) - 20)) \cdot (\frac{t(k)-20}{10})$
3) **Sustained Fault** ($t(k) > 30$s): $\Lambda(:,k) = [0.5;0.5;0.5]$,
   Oscillatory disturbance,
   $f_{osc} = [30;30;30] \cdot \sin(2\pi \cdot 0.5 \cdot (t(k) - 20))$

The fault term f_a includes $(I - \Lambda)\, u_c + f_{osc}$ modeling loss of effectiveness and disturbances.

C. NDI Design for faulty system

The NDI controller cancels nonlinearities in the angular rate dynamics [41], using the nonlinear dynamics $F_1(\omega)$ and control matrix $G_1(\omega)$ defined in Section III-B. The control law is:

$$u_c = G_1{}^{-1}(v - F_1(\omega) - \hat{f}_a) \quad (21)$$

Where $\hat{f}_a$ is the ESO fault estimate, and pseudo-control v:

$$v = \dot{\omega}_d + K_p(\omega_d - \omega) + K_d(\dot{\omega}_d - \dot{\omega}) + K_i \int_0^t (\omega_d - \omega)dt \quad (22)$$

with diagonal gains K_p , K_d , K_i tuned via trial-and-error. Desired rates are:

$$\omega_d(t) = \begin{bmatrix} 0.1 \\ 0.05 \\ -0.1 \end{bmatrix} \sin(0.1t), \dot{\omega}_d(t) \begin{bmatrix} 0.1 \\ 0.05 \\ -0.1 \end{bmatrix} 0.1\cos(0.1t) \quad (23)$$

The final control low is,

$$u_c = G_1{}^{-1}(\dot{\omega}_d + K_p(\omega_d - \omega) + K_d(\dot{\omega}_d - \dot{\omega}) + K_i \int_0^t (\omega_d - \omega)dt - F_1(\omega) - \hat{f}_a) \quad (24)$$

IV. SIMULATION RESULTS

The fault-tolerant control (FTC) framework, combining Nonlinear Dynamic Inversion (NDI) and Extended State Observer (ESO), was evaluated through simulations for the ATLANTE RPA under flaperon faults introduced at t = 20 seconds, as described in Section III-B. The fault injection includes a multiplicative loss of effectiveness (Λ) and oscillatory disturbance (f_{osc}), with a ramp-up phase ($20 < t \leq 30$ seconds) and sustained fault ($t > 30$ seconds). In Fig. 4 the roll, pitch, and yaw rates closely follow their respective desired trajectories, indicating effective tracking performance. The NDI controller ensures smooth responses with minimal deviation, demonstrating good control authority and stability across all rotational axes.

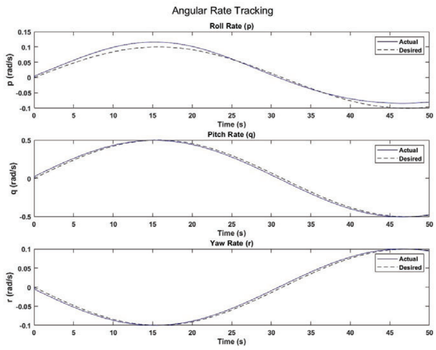

Fig. 4. Angular rates

Control moments in Fig. 5 reflect dynamic fault responses. Roll moment (L) fluctuates between 60 N·m and -20 N·m, stabilizing near 10 N·m, while pitch moment (M) varies between 80 N·m and -60 N·m, adjusting significantly at t = 40 seconds. Yaw moment (N) remains between 20 N·m and -20 N·m, indicating minimal effort for yaw stabilization.

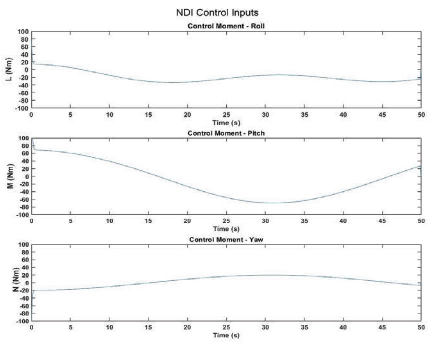

Fig. 5. Control inputs

Fault estimation in Fig. 6 demonstrates ESO accuracy. Roll fault (f_p) spikes to 600 N·m at t = 25 seconds, with the estimate tracking closely despite minor post-spike oscillations. Pitch fault (f_q) reaches 150 N·m, and yaw fault (f_r) drops to 600 N·m, both accurately estimated with slight overshoot.

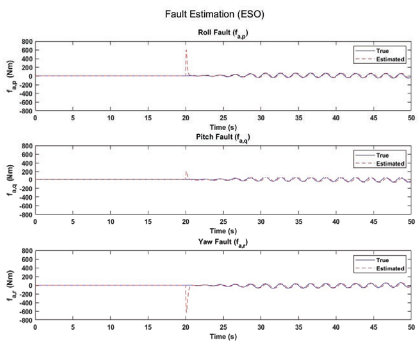

Fig. 6. Faults Estimated vs True

Estimated angular rates in Fig. 7 align closely with actual rates, with minor deviations post-fault, confirming ESO's precision. Fig. 8 shows the control inputs under fault conditions. When the fault occurs around t = 20s, both the commanded (u_c) and effective ($u_c + f_a$) inputs exhibit sharp variations and oscillations as the controller reacts to actuator degradation.

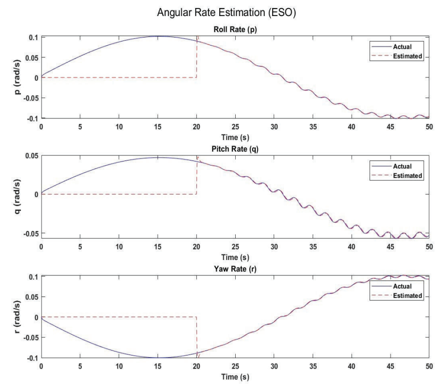

Fig. 7. Rates Estimated vs True

The NDI controller increases its control effort to counteract the reduced actuator effectiveness, while the ESO estimates the fault influence, leading to the eventual stabilization of the control moments.

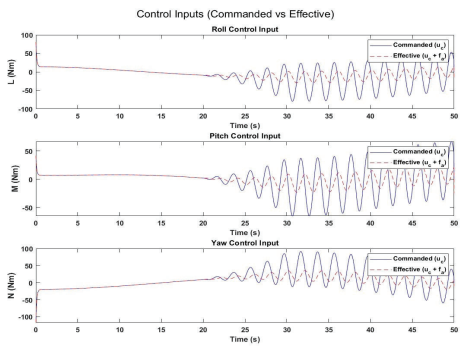

Fig. 8. Control inputs under fault

This behavior demonstrates the controller's capability to maintain effective control performance despite actuator faults. Post-fault recovery Figs. 9–12 highlights FTC effectiveness. In Fig. 9, roll rate (p) tracks the desired rate accurately before t = 20 seconds. At t = 20 seconds, the fault causes an overshoot, with the roll moment (L) spiking to 200 N·m in Fig. 10. FTC activation induces high-frequency oscillations in L, peaking around 200 N·m, as the NDI controller compensates for the fault's impact. By t = 35 seconds, p converges to the desired rate, and L stabilizes, demonstrating robust recovery. The pitch rate (q) tracks well pre-fault, but diverges at t = 20 seconds.

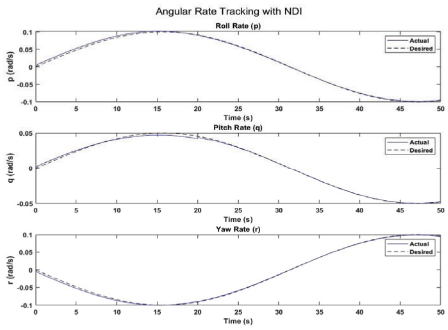

Fig. 9. Rates under fault tolerant control

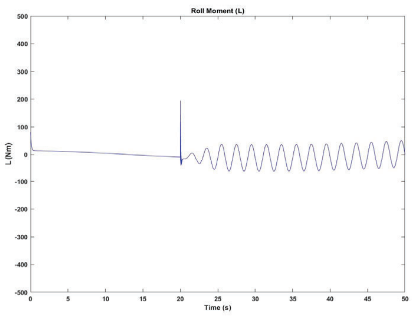

Fig. 10. Roll control input

The pitch moment (M) in Fig. 11 spikes to 200 N·m, followed by high-frequency oscillations post-FTC activation, reflecting dynamic fault compensation. By t = 50 seconds, q achieves near-perfect tracking, and M stabilizes, indicating effective FTC response.

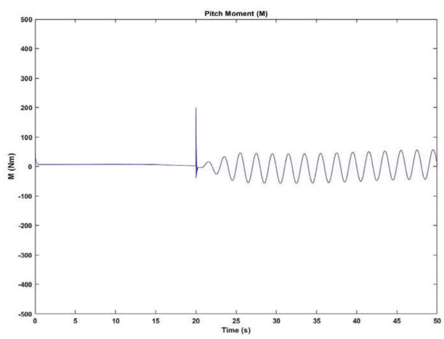

Fig. 11. Pitch control input

The yaw rate (r) undershoots at t = 20 seconds, with the yaw moment (N) in Fig. 12 spiking to 200 N·m. Post-FTC, N exhibits high-frequency oscillations, similar to L and M, as the controller counters the sustained fault (t > 30 seconds). By t = 40 seconds, r converges, and N stabilizes, confirming the framework's ability to manage yaw dynamics under faults.

These results validate the NDI-ESO framework's robustness in tracking desired angular rates, accurately estimating faults, and ensuring stable recovery under flaperon faults across diverse flight conditions.

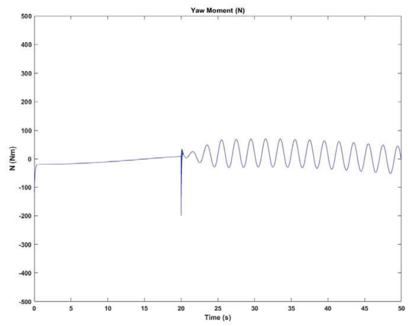

Fig. 12. Yaw control input

V. CONCLUSION

The Fault-Tolerant Control (FTC) system for the ATLANTE Remotely Piloted Aircraft (RPA) effectively mitigates flaperon faults through the integration of Nonlinear Dynamic Inversion (NDI) and Extended State Observer (ESO), as detailed in Section III. The ESO accurately estimates angular rates ($\omega = [p,q,r]^T$) and flaperon faults (f_a), enabling rapid fault detection under the fault injection mechanism described in Section III-B . The NDI controller ensures precise tracking of desired roll, pitch, and yaw rates, with control inputs exhibiting transient spikes up to ±200N · m that settle with damped oscillations, demonstrating robust fault compensation. Simulation results in Section IV validate the system's stability and tracking accuracy, confirming its efficacy in managing flaperon faults across diverse flight conditions.

Future work will focus on enhancing the robustness and real-world applicability of the proposed FTC system through experimental validation on a physical aircraft under realistic disturbances. Further developments include extending the ESO for multi-fault estimation, refining the NDI for adaptive control allocation, and integrating advanced techniques such as adaptive control, model predictive control, and neural network– based fault prediction. These enhancements aim to ensure efficient, reliable, and fault-resilient operation in complex flight conditions.

REFERENCES

[1] Airbus Defence and Space, “ATLANTE: Tactical fixed-wing multirole UAS for maximized operational capability and mission flexibility,” Toulouse, France, 2014.

[2] Cassidian, “ATLANTE: Tactical unmanned aerial system for national security,” Unterschleißheim, Germany, 2014.

[3] H. Alwi and C. Edwards, “An adaptive sliding mode differentiator for actuator oscillatory failure case reconstruction,” Automatica, vol. 49, no. 2, pp. 642–651, 2013.

[4] H. Alwi and C. Edwards, “Robust fault reconstruction for linear parameter varying systems using sliding mode observers,” in Proc. Amer. Control Conf. (ACC), 2015.

[5] H. Jiang and B. Jiang, “Adaptive sliding mode observer-based fault diagnosis for FCS,” in Proc. Int. Conf. Electric Information and Control Eng., 2017.

[6] Y. Guo, B. Jiang, and Y. Zhang, “A novel robust attitude control for quadrotor aircraft subject to actuator faults and wind gusts,” IEEE/CAA J. Autom. Sinica, vol. 5, no. 1, pp. 292–300, 2018.

[7] R. Wang et al., “An actuator fault detection and reconstruction scheme for hex-rotor unmanned aerial vehicle,” IEEE Trans. Control Eng. Pract., vol. 72, pp. 1–10, 2018.

[8] C. Hajiyev and F. Caliskan, “Sensor and control surface/actuator failure detection and isolation applied to flight dynamics,” Aircraft Eng. Aerosp. Technol., vol. 77, no. 3, pp. 1–10, 2005.

[9] Z. Zhengdao and Z. Weihua, “Neural network-based fault detection and identification for fighter control surface failure,” in Proc. Chinese Control and Decision Conf., China, 2009, pp. 1–6.

[10] D. G. Dimogianopoulos, J. D. Hios, and S. D. Fassois, “Aircraft fault detection and identification by stochastic functionally pooled modelling of relationships among attitude data,” J. Aerosp. Eng., vol. 31, no. 4, pp. 1–10, 2018.

[11] R. Hallouzi and M. Verhaegen, “Subspace predictive control applied to fault-tolerant control,” J. Guid. Control Dyn., vol. 31, no. 4, pp. 1–10, 2008.

[12] M. Taimoor and A. Li, “Adaptive strategy for fault detection, isolation and reconstruction of aircraft actuators and sensors,” J. Intell. Fuzzy Syst., vol. 38, no. 1, pp. 1–10, 2020.

[13] P. Lu, E. Kapen, and C. Visser, “Aircraft fault-tolerant trajectory control using incremental nonlinear dynamic inversion,” IEEE Trans. Control Eng. Pract., vol. 57, no. 9, pp. 126–141, 2016.

[14] Y. Yu and L. Wang, “Adaptive fault-tolerant finite-time flight-path angle control for aircraft systems with unknown deadzone and actuator faults,” IEEE Access, vol. 12, pp. 1–10, 2024.

[15] S. Liu, S. Sipeng, and W. Lyu, “Observer-based incremental backstepping sliding-mode fault-tolerant control for blended-wing-body aircraft,” IEEE Trans. Control Eng. Pract., vol. 25, no. 1, pp. 1–11, 2017.

[16] C. Li, T. Zhang, and J. Yang, “Attitude control of aircraft using only synthetic jet actuators when stall occurs,” IEEE Access, vol. 6, pp. 1–10, 2018.

[17] J. O. Ventura, D. B. Morales, J. P. O. Oliver, and E. S. E. Quesada, “Dynamic sliding mode control with PID surface for trajectory tracking of a multirotor aircraft,” IEEE Access, vol. 11, pp. 1–10, 2023.

[18] X. Xiang-rong and Z. Yang, “Research on the variable structure control for the aircraft anti-skid braking systems,” in Proc. Chinese Control and Decision Conf., Yantai, China, 2008, pp. 1–6.

[19] B. Yu, H. Ke, W. Shu, and T. Zhang, “A novel control scheme for aircraft engine based on sliding mode control with acceleration/deceleration limiter,” IEEE Access, vol. 7, pp. 1–10, 2019.

[20] T. Lombaerts, H. O. Huisman, and Q. P. Chu, “Nonlinear reconfiguring flight control based on on-line physical model identification,” J. Guid. Control Dyn., vol. 32, no. 3, pp. 727–748, 2009.

[21] Q. Tan et al., “Reconfigurable nonlinear dynamic inversion for attitude control of a structurally damaged aircraft,” IEEE Access, vol. 8, pp. 1–10, 2020.

[22] N. Tanaka, S. Suzuki, K. Masui, and H. Tomita, “Restructurable guidance and control for aircraft with failures considering gust effects,” J. Guid. Control Dyn., vol. 29, no. 4, pp. 1–10, 2006.

[23] B. Lu, J. Ma, and Z. Zheng, “Adaptive closed-loop control allocation-based fault-tolerant flight control for an over actuated aircraft,” IEEE/CAA J. Autom. Sinica, vol. 6, no. 1, pp. 1–10, 2019.

[24] T. R. Shearwood, M. R. A. Nabawy, W. J. Crowther, and C. Warsop, “Coordinated rollout of conformal finless flying wing aircraft,” IEEE Access, vol. 11, pp. 1–10, 2023.

[25] M. Gopinathan, J. D. Boskovic, R. K. Mehra, and C. Rago, “A multiple model predictive scheme for fault-tolerant flight control design,” in Proc. 37th IEEE Conf. Decision and Control, Tampa, FL, USA, 2000, pp. 1–6.

[26] J. M. Maciejowski and C. N. Jones, “MPC fault-tolerant flight control case study: FLIGHT 1862,” in Proc. IFAC Fault Detection, Supervision and Safety of Tech. Processes, Washington, DC, USA, 2003, pp. 1–6.

[27] J. A. DeCastro, L. Tang, and B. Zhang, "A safety verification approach to fault-tolerant aircraft supervisory control," in AIAA Guid., Navig., Control Conf., Portland, OR, USA, Aug. 2011, pp. 1–6.

[28] J. Roskam, Airplane Design, Part 6. Lawrence, AR, USA: Roskam Aviation Engineering Corporation, 1987.

[29] E. Torenbeek, Synthesis of Subsonic Airplane Design, 1st ed. Delft, The Netherlands: Delft Univ. Press, 1976.

[30] U.S. Department of Defense, "Flying qualities of piloted aircraft," 1997.

[31] J. Roskam, Airplane Flight Dynamics and Automatic Flight Controls. Lawrence, AR, USA: DAR Corporation, 2001.

[32] M. Baarspul, "A review of flight simulation techniques," Prog. Aerosp. Sci., vol. 26, no. 1, pp. 1–10, 1990.

[33] L. Garc´ıa-Hernandez´ et al., "Developing models for future real-time platforms: Virtual simulation and design of new components and systems for aircraft and remotely piloted aircraft systems," in Proc. IEEE Int. Conf. Ind. Technol., Spain, 2015, pp. 1–6.

[34] M. G. Perhinschi, M. R. Napolitano, and G. Campa, "A simulation environment for design and testing of aircraft adaptive fault-tolerant control systems," Dept. Mech. Aerosp. Eng., West Virginia Univ., Morgantown, WV, USA, 2010.

[35] R. E. McFarland, "Finite element aircraft simulation of turbulence," NASA Tech. Memo., Moffett Field, CA, USA, 1997

[36] A. O'Connor and D. Kearney, "Evaluating the effect of turbulence on aircraft during landing and take-off phases," Int. J. Aviat. Aeronaut. Aerosp., vol. 11, no. 1, pp. 1–10, 2024.

[37] Y. Fan, "Analysis of influence of clear air turbulence on aircraft," J. Transp. Technol., vol. 6, no. 2, pp. 45–52, 2018.

[38] L. Garc´ıa-Hernandez, C. Cuerno-Rejado, and M. P´ erez-Cort´ es, "Fault-´ tolerant certifiable control for a V-tail remotely piloted aircraft system," IEEE J. Autom. Sinica, vol. 4, no. 4, pp. 616–625, 2017.

[39] P. E. Purser and J. P. Campbell, "Experimental verification of a simplified vee-tail theory and analysis of available data on complete models with vee-tails," Nat. Adv. Comm. Aeronaut. (NACA), Langley Field, VA, USA, 2006.

[40] International Civil Aviation Organization (ICAO), "Aircraft operations— flight procedures," Montreal, BC, Canada, 2016.

[41] X. Ma, S. Liu, and H. Cheng, "Civil aircraft fault-tolerant attitude tracking based on extended state observers and nonlinear dynamic inversion," J. Syst. Eng. Electron., vol. 33, no. 2, pp. 180–187, Feb.2022.